Discussion on DQMOM to solve a bivariate population balance equation applied to a grinding process

Alain Liné [a], Christine Frances [b,*]

[a] *LISBP, Université de Toulouse, CNRS, INRA, INSA, Toulouse, France*
[b] *Laboratoire de Génie Chimique, Université de Toulouse, CNRS, INPT, UPS, Toulouse, France*

A B S T R A C T

A bivariate population balance equation applied to a grinding process is implemented in a model (PBM). The particles are simultaneously characterized by their size and their mechanical strength, expressed here by the minimum energy needed to break them. PBM is solved by the Direct Quadrature Method of Moments (DQMOM). The mixed moments of the distribution are expressed by the quadrature form of the population density defined for one order (N) and incorporating the weights and the abscissas defined for the two properties. The effect of the quadrature order ($N = 2, 3, 4$) and the selected set of the $3N$ moments needed to solve the system on the accuracy of the results is discussed. For a given order of the quadrature, the selected set of the initial mixed moments slightly affects first the weights and abscissas derived from the initial particle distribution. The set of moments also affects the precision of the moments calculated versus time but only those having high orders in relation with the respective range of the solid properties considered. Problems of convergence and significant differences in the predicted mixed moments are also observed when the order of the quadrature is equal to 2. However, the changes of a bivariate distribution versus time applied to a grinding process are well predicted using the DQMOM approach, choosing a number of nodes equal to 3, associated with a smart selection of the moment set, incorporating all the moments of interest.

1. Introduction

Particulate process models are currently based on population balance equations either in homogenous conditions or heterogeneous systems combining CFD modeling. They allow tracking the temporal evolution, and eventually the spatial change, of the population density or the particle distribution during continuous processes (growth, dissolution, coating, grinding, erosion, …) or discrete events (nucleation, aggregation, rupture, flocculation, …) [1–4]. The solid phase characteristics are described by the particle size or volume. More rarely, two or more properties for the discontinuous phase are considered (such as surface/volume, size/composition, or volume/size [5–7]. Bivariate or multidimensional population balance equations have particularly been developed to describe solid properties during crystallization [8–10] or precipitation processes [11–12], as well as for granulation [13], coagulation and sintering processes [14] or even more recently to describe the depolymerization of branched polymers [15]. The population balance models applied to grinding processes usually allow describing the transient change of the particle size distribution. However, other properties of the solid phase can be important to drive the process, as morphological or physical properties. In this work, we use a population balance equation (PBE) in which the particles are simultaneously characterized by their size and their mechanical resistance. The particle resistance, expressed as the minimal energy needed to break the particles, also called the breakage energy, can be evaluated from fracture tests usually done on individual particles as with the Hopkinson pressure bar or the Ultrafast Load Cell [16–17]. Nano-indentation tests, developed more recently, are also performed on single particles. Such tests allow performing the analysis of mechanical properties on fine particles or even in the submicron particle size range [18].

The PBE in homogeneous conditions is solved here using the Direct Quadrature Method of Moments (DQMOM) since one of its advantages is to easily take into account of several properties for the solid phase [19–22,15]. The mixed moments of the population density are given by the quadrature approximation incorporating the weights and abscissas with respect to the two solid properties. The weights and abscissas are defined for a given number N of nodes. In the studied case, based on Crespo analysis [23], the two properties of the solid phase are dependent since the breakage energy is conditioned by the particle size. The PBE could then be solved with a conditional quadrature method of moments [24]. However, in order to keep things generic, the method has been developed using the more general DQMOM approach. Then it could be extended to track any solid properties, either dependent or not. The validation of the DQMOM method and the

* Corresponding author.
  E-mail address: christine.frances@ensiacet.fr (C. Frances).

interest of a bivariate approach considering both the particle size and the breakage energy compared to the monovariate approach have been discussed in a previous paper [25]. The objective of the present contribution is to discuss the effect of the number of nodes and the mixed moments selected set needed to close the problem on the precision of the simulated results.

2. Grinding process modeling

2.1. DQMOM general equations

The homogeneous equation of population balance considering two properties for the solid phase can be written as follows by introducing the particle-size energy distribution $f(x,e,t)$, which represents the mass fraction of particles characterized by size x and fracture energy e at instant t:

$$\frac{\partial f(x,e,t)}{\partial t} = S(x,e,t). \tag{1}$$

The right hand side of the equation represents all the birth and death terms. In case of a pure breakage process, it comprises only two terms, the first one expresses the disappearance of particles due to their breakage in smaller pieces and the second one the apparition of fragments of properties x and e due to the breakage of larger particles:

$$\begin{aligned}\frac{\partial f(x,e,t)}{\partial t} = &-a(x,e)\,f(x,e,t)\\ &+\int_{0}^{+\infty}\!\!\int_{x}^{+\infty} a(x_0,e_0)\,b(x,e,x_0,e_0)\,f(x_0,e_0,t)\,dx_0\,de_0.\end{aligned} \tag{2}$$

$a(x,e)$ is the selection function, it describes the rate at which particles of size x and breakage energy e are broken. The breakage function $b(x,e,x_0,e_0)$ represents the probability to obtain fragments of properties (x,e) after a breakage event of particles characterized by a size x_0 and a breakage energy e_0.

The quadrature methods of moments used to solve the population balance equations are based on the approximation of the density function by the Gaussian quadrature:

$$f(x,e,t) = \sum_{i=1}^{N} w_i(t)\,\delta(x(t)-x_i(t))\,\delta(e(t)-e_i(t)) \tag{3}$$

where N is the order of the quadrature, i.e. the number of nodes i, x_i is the first property of the node (the particle size), e_i is the second property of the node (the particle minimum energy for breakage), w_i is the node weight and δ the Dirac function. x_i and e_i are also called the abscissas.

If the discrete decomposition Eq. (3) is injected into Eq. (1), one obtains the following equation:

$$\begin{aligned}&\sum_{i=1}^{N}\delta(x-x_i)\,\delta(e-e_i)\,u_i-\sum_{i=1}^{N}\delta'(x-x_i)\delta(e-e_i)\\ &(v_i-x_iu_i)-\sum_{i=1}^{N}\delta(x-x_i)\,\delta'(e-e_i)\,(z_i-e_iu_i)\\ &= S(x,e,t).\end{aligned} \tag{4}$$

u_i, v_i and z_i being respectively the transient changes of the weights, the weighted sizes and weighted energies defined as:

$$\frac{\partial w_i}{\partial t} = u_i \tag{5}$$

$$\frac{\partial(w_ix_i)}{\partial t} = v_i \tag{6}$$

$$\frac{\partial(w_ie_i)}{\partial t} = z_i. \tag{7}$$

After transformation of Eq. (4) by the moments; the mixed moments being defined by:

$$m_{kl}(t) = \iint_{-\infty}^{+\infty} x^k e^l\,f(x,e,t)\,dx\,de = \sum_{i=1}^{N} w_i\,x_i^k\,e_i^l. \tag{8}$$

One obtains:

$$\begin{aligned}&\sum_{i=1}^{N}\left[(1-k-l)x_i^k e_i^l u_i + kx_i^{k-1} e_i^l v_i + lx_i^k e_i^{l-1} z_i\right]\\ &= -\sum_{i=1}^{N} w_i x_i^k e_i^l a_i + \sum_{i=1}^{N} a_i \overline{b}_l^{kl} w_i\end{aligned} \tag{9}$$

with:

$$a_i = a(x_i,e_i) \tag{10}$$

and:

$$\overline{b}_i^{kl} = \iint_{0}^{\infty} x^k\,e^l\,b(x,e,x_i,e_i)\,dx\,de. \tag{11}$$

Eq. (9) is an algebraic system with $3N$ unknowns: $u_1, ..., u_N, v_1, ..., v_N, z_1, ..., z_N$ which are themselves solutions of the ordinary differential equations defined by Eqs. (5), (6) and (7).

2.2. Specific equations for the present case

Although the two solid properties (particle size and breakage energy) have been mathematically treated as if they were independent, the breakage energy is assumed in this work to be dependent on particle

Approximated initial mixed moments (Eq. (19))	m00	m10	m01	m20	m11	m02	m30	m21	m12	m03	m40	m31	m22	m13	m04
	1.00	2.99	3.06	9.25	9.72	14.84	29.25	31.55	49.40	111.80	94.68	104.71	167.92	388.85	1283.33
Back calculated initial mixed moments (Eq. (8))	m00	m10	m01	m20	m11	m02	m30	m21	m12	m03	m40	m31	m22	m13	m04
Moments set															
m00 m10 m01 m20 m11 m02 +															
Set 1: m30 m03 m22	1.00	2.99	3.06	9.25	9.72	14.84	29.25	31.45	49.69	111.80	94.30	103.44	167.92	384.41	1035.22
Set 2: m30 m21 m03	1.00	2.99	3.06	9.25	9.72	14.84	29.25	31.55	50.36	111.80	94.56	104.48	173.08	393.75	1029.50
Set 3: m30 m12 m03	1.00	2.99	3.06	9.25	9.72	14.84	29.25	31.40	49.40	111.80	94.09	102.87	165.70	380.57	1038.74
Set 4: m30 m21 m12	1.00	2.99	3.06	9.25	9.72	14.84	29.25	31.52	49.40	96.04	94.03	103.51	165.84	326.16	690.45
Set 5: m21 m12 m03	1.00	2.99	3.06	9.25	9.72	14.84	29.28	31.51	49.41	111.80	94.33	103.37	165.69	280.02	1042.65
Set 6: m30 m21 m12 m03	0.99	3.03	3.01	9.41	9.81	14.76	29.40	32.00	49.57	112.21	92.44	104.75	166.87	388.89	1282.05
m40 m31 m22 m13 m04															

Table 2
Initial values of weights and abscissas calculated for various selected sets of moments for $N=3$ varying the last moments given the first six ones as $[m_{00}, m_{10}, m_{01}, m_{20}, m_{11}, m_{02}]$

Moments set m00 m10 m01 m20 m11 m02 +...	Weights			Abscissas-size			Abscissas-energy		
Set 1: m30 m03 m22	0.41	0.49	0.10	2.38	3.41	3.47	1.90	2.63	10.06
Set 2: m30 m21 m03	0.50	0.40	0.10	2.50	3.48	3.57	2.13	2.46	9.94
Set 3: m30 m12 m03	0.34	0.57	0.09	2.28	3.35	3.43	1.75	2.66	10.14
Set 4: m30 m21 m12	0.30	0.48	0.22	2.21	3.30	3.42	1.75	1.88	7.47
Set 5: m21 m12 m03	0.31	0.59	0.10	2.21	3.34	3.42	1.63	2.70	10.22
Set 6: m30 m21 m12 m03 m40 m31 m22 m13 m04	0.36	0.61	0.02	2.73	3.27	3.58	0.71	4.05	15.63

size with respects to experimental data reported in the literature [23]. Indeed, the minimum energy needed to break particles is usually evaluated from single-particle fracture tests [16–17]. This leads to scattered data due to the particle structure heterogeneity and to the presence of an initial crack pattern inside the particles. The fracture energy also depends on particle size and tests are usually conducted on calibrated or sieved particles. The experimental results are then interpreted using statistical tools. The formulation adopted by Tavares and King [16] was used; it expressed the fracture probability by a log-normal distribution:

$$P(E|x) = \frac{1}{2}\left[1 + erf\left(\frac{\ln(E/E_{50})}{\sqrt{2\sigma_E^2}}\right)\right] \tag{12}$$

where E is the mass-specific particle fracture energy, equal to the

particle fracture energy divided by the mass of a particle. E_{50} and σ_E are the median and geometric variance of the distribution, respectively. They depend on material properties. Data reported by Tavares and King [16] relative to irregular quartz particles were used. In the present case, the units considered for particle size and fracture energy are respectively mm and mJ and the grinding time is given in min.

The energy spectrum, assumed to be independent of time, is thus given by:

$$f(e|x) = \frac{exp\left[-\frac{(\ln(e/e_{50}))^2}{2\sigma_E^2}\right]}{e\sqrt{2\pi\sigma_E^2}}. \tag{13}$$

Moreover, the following selection and breakage functions have been used. More details on the case studied could be found in Frances and Liné [25]:

$$a(x,e) = A_0\left(\frac{x}{x_{max}}\right)^{a_0}\left[exp\left(-\frac{e}{e_*}\right)\right] \tag{14}$$

$$b(x,e,x_0,e_0) = b(x,x_0)\,b(e|x) = \frac{a_0}{x_0}\left(\frac{x}{x_0}\right)^{a_0-1}\frac{exp\left[-\frac{(\ln(e/e_{50}))^2}{2\sigma_E^2}\right]}{e\sqrt{2\pi\sigma_E^2}}. \tag{15}$$

2.3. Computational details

Population balance equations adapted for DQMOM method have $3N$ unknowns in the bivariate case constituted by the weights and the abscissas for each solid property. $3N$ mixed moments are thus needed
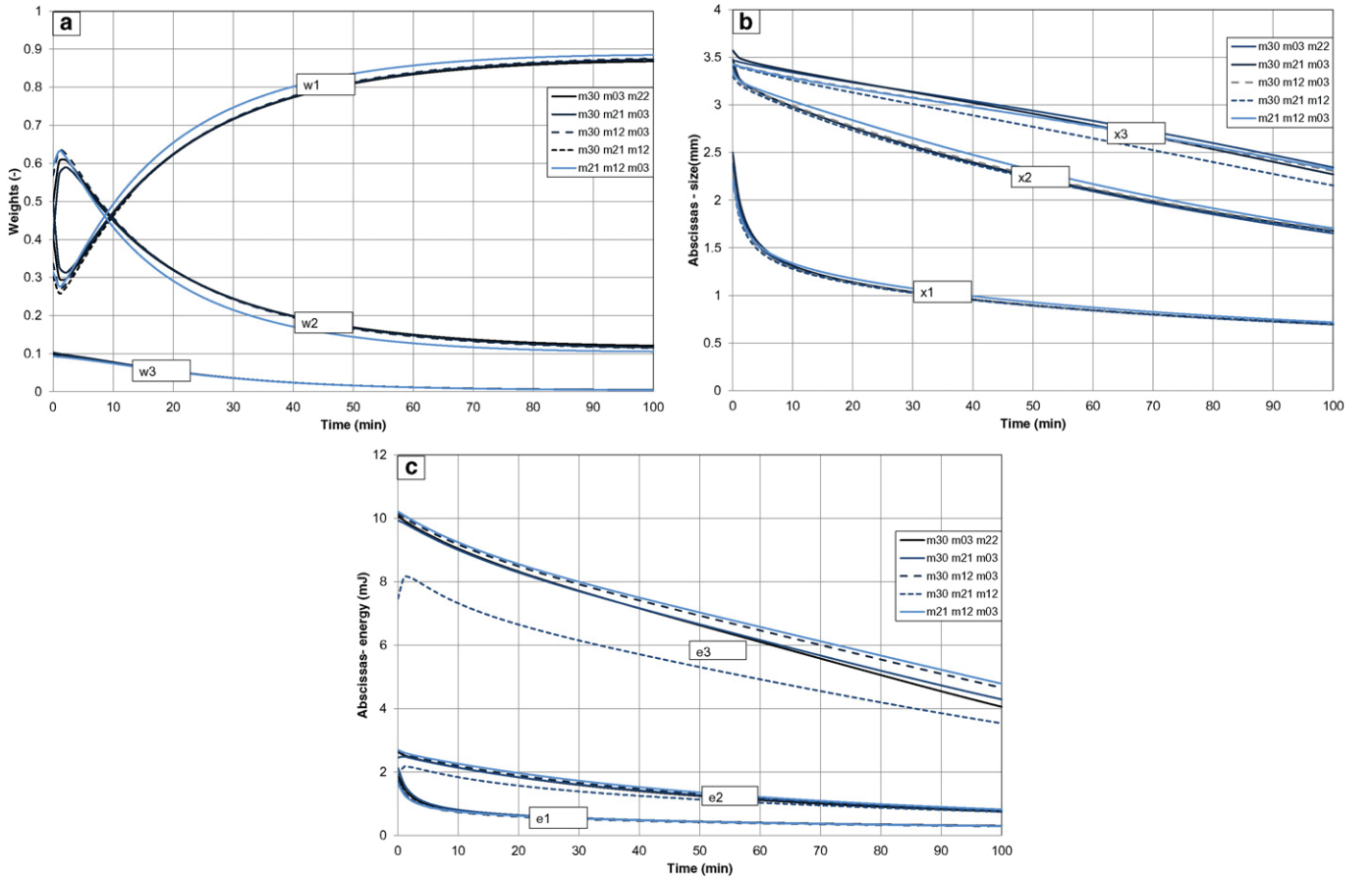
Fig. 1. Change in the weights and abscissas for $N=3$ with different choices for the last three moments given the first six ones as $[m_{00}, m_{10}, m_{01}, m_{20}, m_{11}, m_{02}]$.
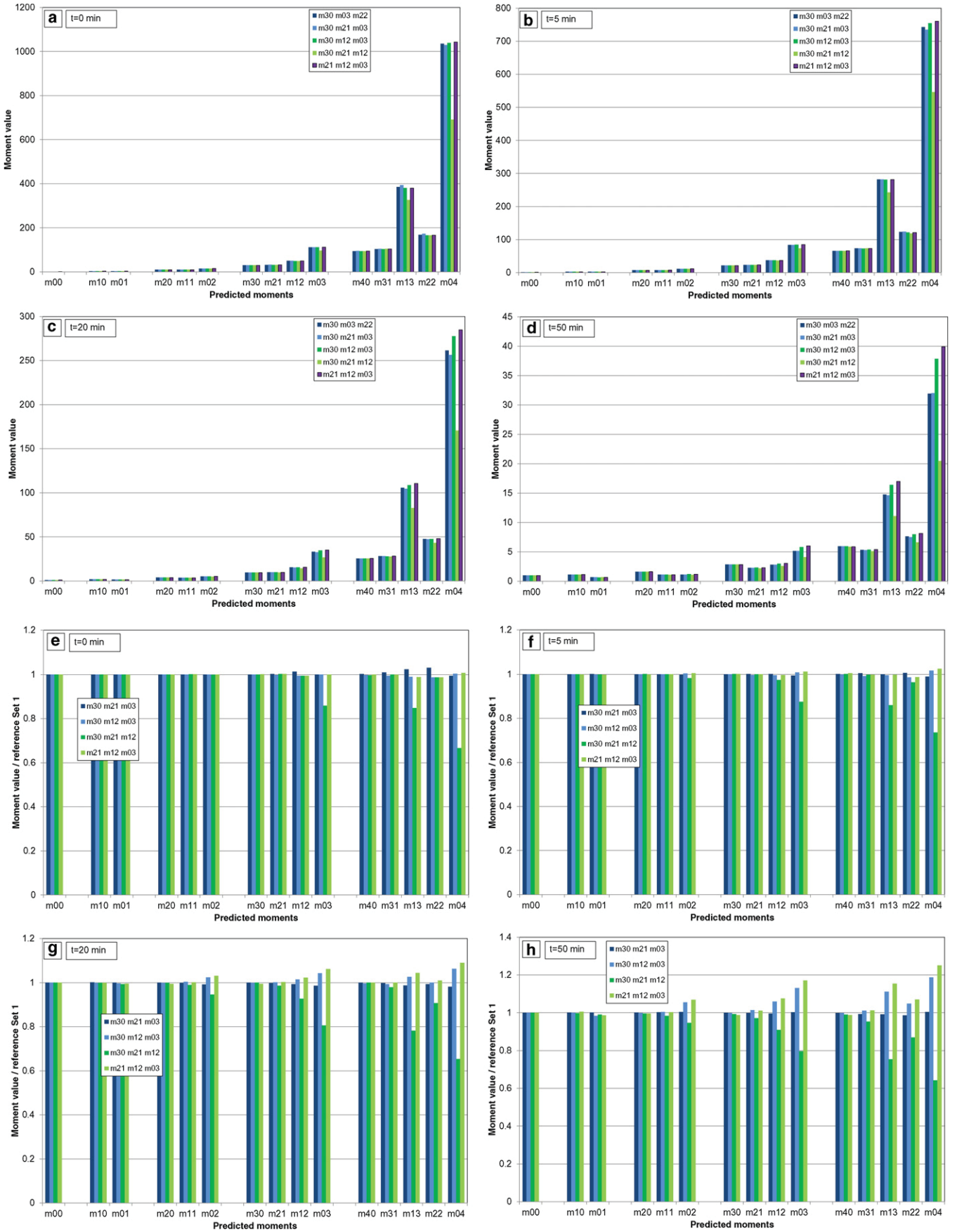
Fig. 2. Change in the predictions of the first mixed moments vs. time obtained by DQMOM with $N = 3$ and different sets, given the first six moments as $[m_{00}, m_{10}, m_{01}, m_{20}, m_{11}, m_{02}]$ and varying the last three ones (panel a: $t = 0$, panel b: $t = 5$ min, panel c: 20 min, panel d: 50 min) and corresponding dimensionless moment values taking the Set 1 as a reference (panel e: $t = 0$, panel f: $t = 5$ min, panel g: 20 min, panel h: 50 min).
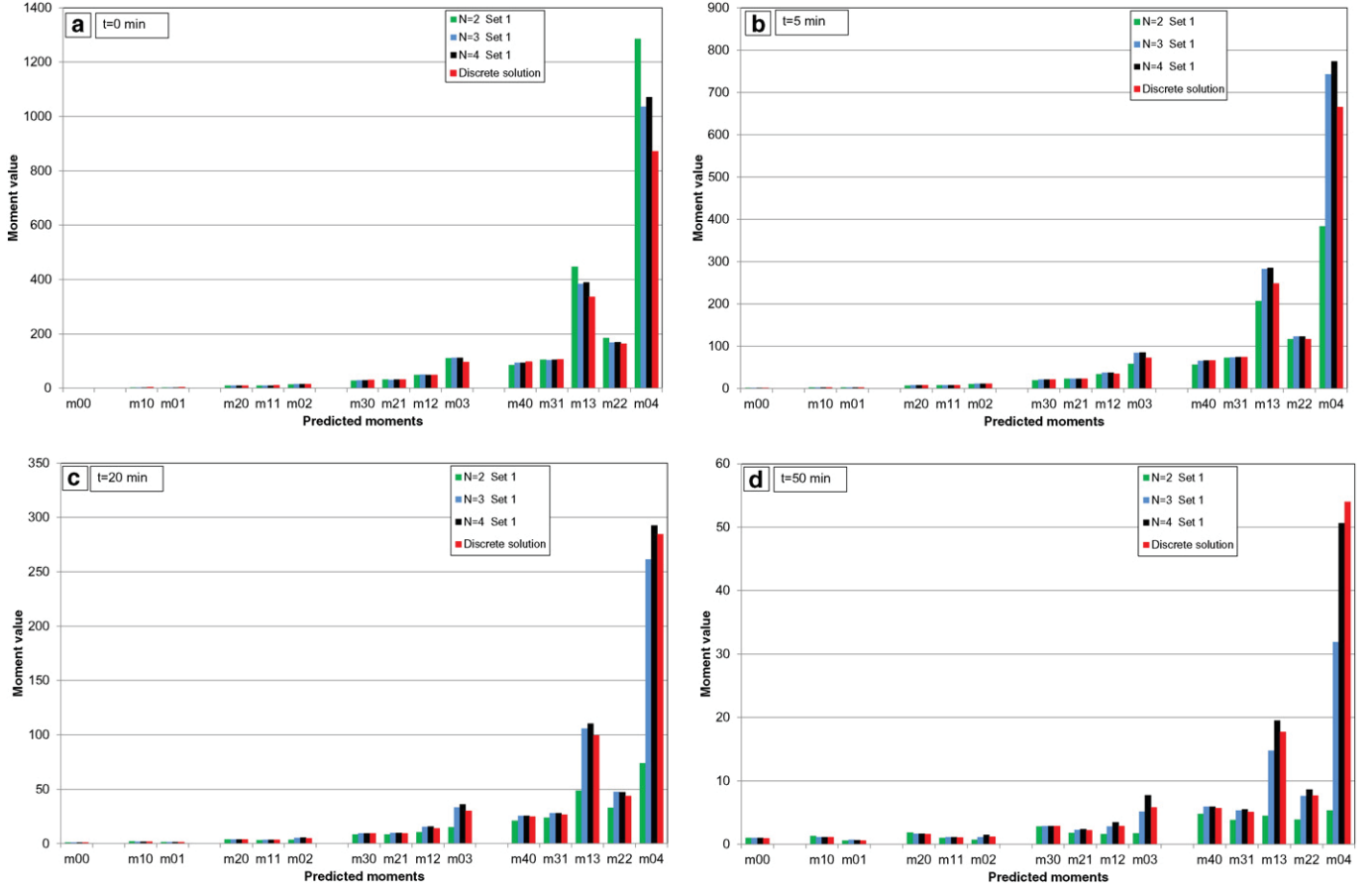
Fig. 3. Change in the predictions of the first mixed moments vs. time obtained by DQMOM with different numbers of nodes and comparison with the discrete solution of the PBE.

to close the system. Computations were performed using Matlab for different selected sets of moments and for different quadrature orders N from 2 to 4. Eq. (9) is written under a matrix form and solved using the matrix division Matlab operator. The solution of this linear ordinary equation contains $3N$ components. These components correspond to the right hand sides of the ordinary differential equations (ODE) given by Eq. (5) to (7). The ODE system was solved using the Ode113 Matlab subroutine.

The initial particle size-energy distribution has to be defined to initialize the code. For the results presented in the following sections, the initial particle size distribution was assumed to be a normal-law with a mean equal to 3 and a standard deviation to 0.5. The energy spectrum was given by Eq. (13) in which the reference parameter e* and the geometric variance energy distribution were taken as $e^* = e_{50}(x = x_{max} = 6 \text{ mm})$ and $\sigma_E^2 = 0.345$. The kinetic parameters of Eq. (14) were also kept constant ($A_0 = 0.5 \text{ min}^{-1}; a_0 = 2$).

Using the DQMOM approach, the code must be initialized by the weights and abscissas of the initial distribution. In the monovariate case, such quantities can be easily determined from the first moments of the particle distribution using the Product-Difference algorithm [26]. In the bivariate case, the determination of the weights and abscissas is not so simple and may be a key point in the numerical procedure. In the present work, the initialization was performed using the same mixed moments (at the initial time) as those considered for each chosen set and solving by the least squares method (Matlab subroutine *lsqnonlin*) the non-linear system defined by the following equations:

$$\frac{\sum_{i=1}^{N} w_i \, x_i^k \, e_i^l}{m_{kl}(0)} - 1 = 0 \tag{16}$$

(k,l) scanning the $3N$ couples of the selected set of moments. The initial mixed moments were calculated by the double quad method using the

Table 3
Comparison of DQMOM predictions for different numbers of nodes with the discrete solution

Initial mixed moments	m30	m21	m12	m03	m40	m31	m22	m13	m04
Discrete solution	29.81	31.81	47.75	96.01	97.06	106.16	163.18	335.68	870.79
% Error N = 2 Set 1	−7.2	−0.8	+3.4	+15.0	−11.9	−0.8	+12.9	+33.1	+49.5
% Error N = 3 Set 1	−1.9	−1.1	+4.1	+16.4	−2.8	−2.6	+2.9	+14.5	+18.9
% Error N = 4 Set 1	−1.9	−0.8	+3.4	+16.5	−2.8	−1.4	+3.6	+15.9	+23.0
Mixed moments at 50 min	m30	m21	m12	m03	m40	m31	m22	m13	m04
Discrete solution	2.84	2.19	2.86	5.84	5.69	5.06	7.66	17.69	53.98
% Error N = 2 Set 1	−2.5	−18.1	−44.3	−70.5	−16.5	−24.8	−49.1	−74.7	−90.1
% Error N = 3 Set 1	+1.3	+3.6	−1.0	−11.9	+4.4	+5.6	−0.5	−16.7	−40.9
% Error N = 4 Set 1	+1.7	+8.4	+20.7	+32.5	+4.4	+8.4	+12.6	+10.3	−6.3
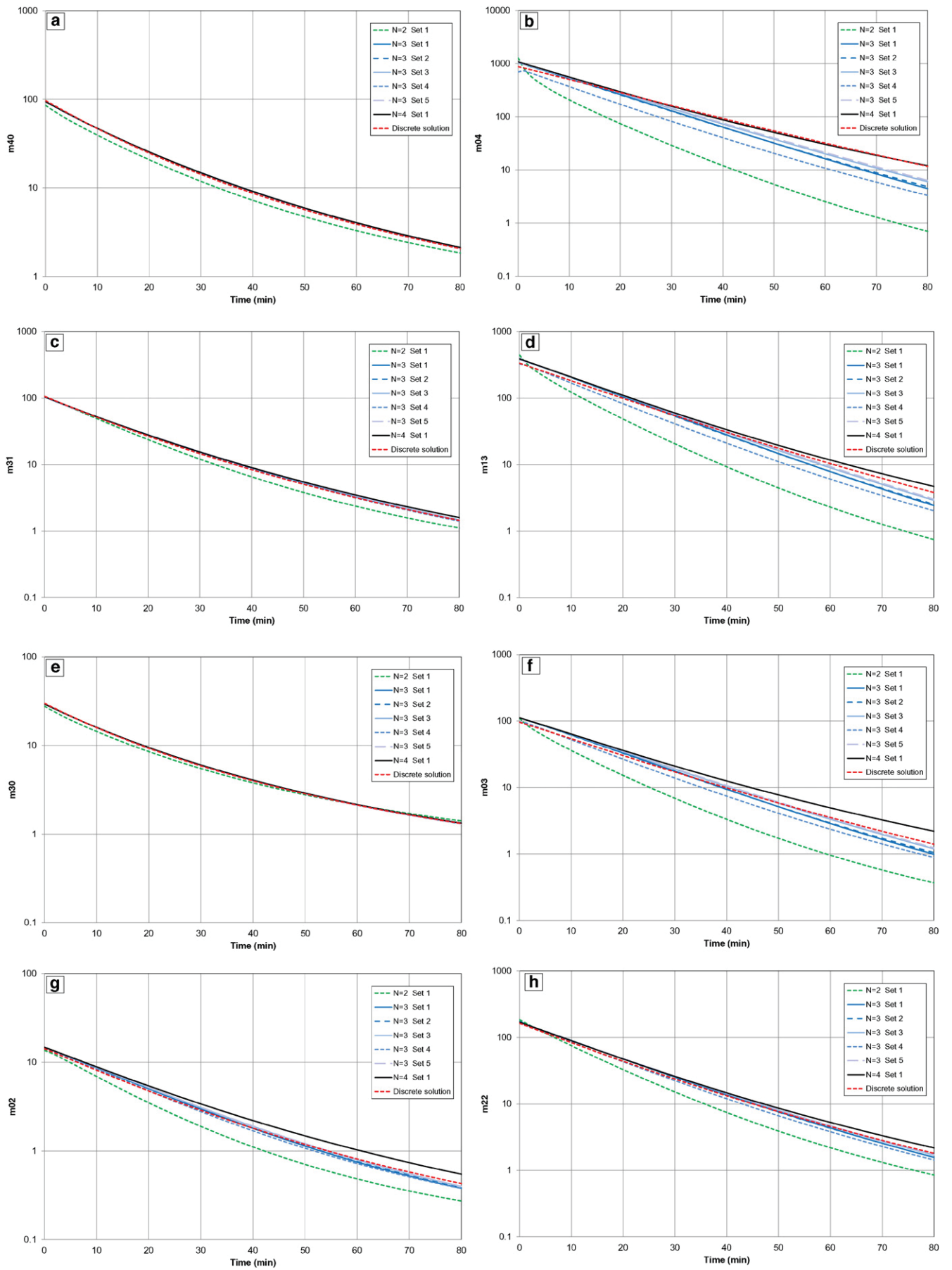
Fig. 4. Predictions of some mixed moments by DQMOM with different numbers of nodes and different sets for $N = 3$ and comparison with the discrete solution.

Table 4
Evaluation of the process time-scale (in min) as function of the number of nodes

N	τ_{k1}	τ_{k2}	τ_{k3}	τ_{k4}	δ_1	δ_2	δ_3	δ_4
N2 Set 1	33.3	18.5	13.7	11.6	20.8	15.9	–	–
N3 Set 1	30.3	19.2	15.6	13.5	23.8	18.9	16.9	15.1
N4 Set 1	30.3	19.6	15.9	13.7	23.2	19.6	17.8	15.4

Matlab subroutine *dblquad*. On the base of the specific equations used for the studied case, the mixed moments are defined by:

$$m_{kl} = \iint_0^\infty f(x,e,t)\, x^k\, e^l\, dx\, de = \iint_0^\infty f(e|x,t)\, f(x,t)\, x^k\, e^l\, dx\, de. \tag{17}$$

The fracture probability being given by Eq. (12), the breakage energy can be written as:

$$e = e_{50}\, exp\left(\sqrt{2\sigma_E^2}\; erfinv(2P - 1) \right). \tag{18}$$

Introducing the variable change $s = 2P\text{-}1$ in Eq. (17), the following simplified expression for the mixed moments can finally be derived:

$$m_{kl} = \iint_0^\infty f(x,t)\, x^k\, e^l\, dx\, dP. \tag{19}$$

The initial mixed moments were then calculated using the Matlab *dlbquad* subroutine, setting the minimum and maximum integral bounds respectively at $x_{\min} = 0$ and $x_{\max} = 6$ mm for the particle size and $P_{\min} = 0.00001$ and $P_{\max} = 0.99999$ for the fracture probability. Some mixed moments are reported on Table 1.

A discrete solution of the population balance equation was also used to compare the results obtained with DQMOM varying the selected sets or the quadrature order. For that purpose, discrete forms for the selection and breakage functions were introduced in the PBE as suggested by Crespo [23]. The problem was then solved by considering one hundred and fifty intervals for the particle size, ranging between 0 and 6 mm and one hundred and fifty intervals for the energy range. The energy range was chosen to obtain a breakage probability between 0 and 1 for each size class. More information on the discrete solution and numerical details can be found in Frances and Liné [25].

3. Results and discussion

3.1. Effect of the selected set of mixed moments

Theoretically, the choice of moments can be done arbitrarily as long as it results to a non-singular matrix derived from Eq. (9) whatever the values of the weights and abscissas considered. General rules to select an optimal set of moments were given by Fox [27]. Thus, it is recommended to include all the lower-order mixed moments of a particular global order n (a mixed moment m_{kl} having a global order n defined by $n = k + l$) before adding moments of higher order and treating equally all the internal coordinates. Following Fox [27], it is known that in the general case (non-conditional properties), there is no optimal set when the number of nodes is notably equal to 2 or 3. However, although there is no optimal set in these cases, it is possible to select a valid one, which allows building a successful quadrature approximation. For example, if $N = 3$ and if the number of internal coordinates is equal to 2, nine mixed moments must be chosen to solve the system. It is recommended to choose first all the moments with a global order less than or equal to two, i.e. $(m_{00}, m_{10}, m_{01}, m_{20}, m_{11}, m_{02})$ and to select for the remaining needed moments three moments among the four of global order three. However, whatever the choice, the two internal coordinates will not be treated equally. The only way to respect this last condition is to choose two symmetric moments of global order three and one symmetric moment (m_{22}) of global order 4.

In this section the effect of the selected set of moments with $N = 3$ on the simulated results is discussed. Several sets, defined as valid ones as discussed before, were tested. They are listed in Table 1 and in Table 2 as well. Table 1 reports for the different selected sets, the initial values of some mixed moments back calculated with the quadrature based formula (Eq. (8)) in which were considered the weights and abscissas recovered for each selected set solving the non-linear system (Eq. (16)) and reported in Table 2. It can be observed that the initial values of the mixed moments can slightly differ from the values approximated by the double quad method and can also be different choosing one set or another. All the mixed moments of a global order less or equal to 2 approximated by the double quad method or by the quadrature formula whatever the selected set were identical. The differences become more significant considering the mixed moments with a higher global order. Moreover, it can also be noticed that the values of the mixed moments (highlighted values in Table 1) calculated with the quadrature formula are identical to the approximated values when these mixed moments are included in the selected set. The corresponding weights and abscissas obtained for the different selected sets are reported in Table 2. It is again observed that the initial values of the weights and abscissas are slightly different choosing one set or another. Using this procedure the initial weights and abscissas, and consequently the initial mixed moments, are not exactly the same, depending on the selected set.

Another way to initialize the weights and abscissas is to consider an oversized non-linear system (Eq. (16)) choosing a number of mixed moments greater than $3N$. For example, the Set 6 was constructed taking all the first mixed moments of interest having a global order equal or less than 4 (15 mixed moments) as listed in Tables 1 and 2. In that case, quite different values of initial weights and abscissas were obtained (cf. Table 2), comparatively to the previous ones. The initial mixed moments back calculated by the quadrature formula were globally close to the moments approximated by the double quad method but none of them was strictly identical to the approximated corresponding value (cf. Table 1). Considering the initial values of weights and abscissas reported on Table 2 for Set 6 and selecting then one set or another (Set 1 to Set 5), the initial mixed moments were obviously identical but some problems occurred using the DQMOM solving code (negative abscissas recovered). So the first procedure to initialize the code was applied in the following results.

The evolutions of the weights and abscissas along time are reported on Fig. 1. Globally speaking, the change of the abscissas-size versus time puts in evidence a decrease of the particle size which is obvious with a pure breakage process. Even if it not fully true, if we consider in a simplified view that the three nodes represent three sub-populations of the particles, several observations can be done:

- The weight fraction of the coarser population (w_3) is initially low (around 10%) and it gradually decreases versus time to zero. The grinding kinetics having an order 2 with respect to the particle size ($a_0 = 2$), the higher is the particle size, more rapid is the size decrease.
- Concerning the intermediate and finer sub-populations, their evolutions are quite correlated. The sub-population of the intermediate-size population first increases (may be due to the breakage of the coarser particles) and then decreases to the benefit of the finer population. Inversely, the fraction of the fines seems to decrease during the first minutes of the process before increasing and becoming the main sub-population after ten minutes. In fact, during the first minutes of the process, the fines do not disappear but their characteristic size (which can be approximated by x_1) sharply decreases.
- The change of the abscissas-energy versus time is similar to that of the abscissas-size since in the present case the energy needed for breakage is correlated with the particle size. The higher the particle size, the higher is the minimum energy for breakage in the studied case.

Moreover, the effect of the selected set of moments on the predictions of the weights is not very important, remembering that slight differences were already present at the initial time. The values of the weights recovered for the different selected sets even seem to converge along time, except for those obtained with the Set 5. Considering now the changes of the size and energy abscissas versus time, it can be concluded that the effect of the selected set of moments is rather weak for the Sets 1, 2, 3 and 5. Some differences can be observed on the evolution of the third abscissa. The difference is more pronounced for the Set 4 but this was already true at the initial time as mentioned before and it tends to lessen versus time. It must be noticed that in Set 4 and Set 5 only one pure moment of global order three (m_{30} or m_{03}) was selected compared to the other selected sets.

The change in the predictions of the first mixed moments for some process times obtained with DQMOM for three nodes and different sets are presented on Fig. 2(a–h). On Fig. 2a to d, the magnitude of the calculated moments is put in evidence. On Fig. 2e to f, the corresponding dimensionless moment values have been reported taking the first selected set of moments as an arbitrary reference in order to emphasize the effect of the selected set on the mixed moments at any time.

It can be observed on Fig. 2 that the moments of global order less than or equal to 2, as well as the pure moments m_{30} and m_{40} are very similar whatever the set chosen. More significant differences appear for moments with a higher global order and more particularly for those having a high order with respect to the second internal coordinate: m_{03}, m_{13}, m_{04}. These differences already exist at the initial time. They are the consequence of the differences on the initial weights and abscissas selecting one set or another as previously indicated and reported in Table 2. The difference between the predictions slightly increases versus time as it is put in evidence on dimensionless moments reported on Fig. 2e to h. This result must be put in relation with the respective range of variation of the two properties. Indeed, the particle size varies between 0 and 6 mm in that example, whereas the breakage energy may take values greater than several tens of mJ. As a consequence, pure moments of order 4 for the second property (m_{04}) are higher than six times the equivalent pure moments for the first property (m_{40}). It must again be noticed that the most discrepancy between the predicted values occurs for those calculated using the Set 4, for which the moment m_{03} is not included in the set.

Globally speaking, the values of the moments differ from one set to another if they are not included in the set of moments used to saturate the degrees of freedom. This limitation was already pointed out by Marchisio and Fox [22]; including one moment of interest in the selected set increases the accuracy of the prediction of this specific moment. The results presented here are also in agreement with Zucca et al. observations [21]. Comparing the values of the moment m_{30} obtained by a Monte Carlo method and a DQMOM method for various sets of moments choosing the last three moments of global order 3, global order 4 or global order 5 given the first six moments as it was done here, they concluded that m_{30} was well predicted only by including moments of global order three in the moment set. So in our example, accurate predictions of moments of global order 4 could only be obtained increasing the number of nodes. For $N = 4$, twelve moments are needed to solve the bivariate PBE. In that case, optimal sets can be used, given the first ten moments as ($m_{00}, m_{10}, m_{01}, m_{20}, m_{11}, m_{02}, m_{30}, m_{21}, m_{12}, m_{03}$) and choosing for the last two ones (m_{40}, m_{04}) or (m_{31}, m_{13}). In each of these two selected sets, all the moments of order 0, 1 2 and 3 moments are selected and the two last ones allow treating equally both properties.

3.2. Effect of the number of nodes

The effect of the number of nodes for N equal to 2, 3, or 4 was also analyzed. In order to analyze the effect of the number of nodes on the calculated results, the change in the predictions of the first mixed moments obtained with DQMOM with different number of nodes from 2 to 4 are reported on Fig. 3 for some specific times. Several sets of moments were tested for a number of nodes equal to 2, for which there is no optimal set to choose. In that case several sets did not allow converging towards a physical solution (prediction of negative abscissas for example). The results reported here for $N = 2$ were obtained choosing the following set: Set 1 = ($m_{00}, m_{10}, m_{01}, m_{11}m_{21}, m_{12}$). Choosing one optimal set or the other for $N = 4$, the convergence towards physical solutions was reached and the predictions were quite similar for all moments having a global order less or equal to two and for pure moments with respect to the first coordinate. As for the case $N = 3$, some differences appear for moments with a higher global order especially for those having a high order with respect to the second internal coordinate. The results presented here for $N = 4$ were obtained with the following set: Set 1 = ($m_{00}, m_{10}, m_{01}, m_{20}, m_{11}, m_{02}, m_{30}, m_{21}, m_{12}, m_{03}, m_{31}, m_{13}$). Moreover, in the histograms of Fig. 3, the results obtained with the Set 1 = ($m_{00}, m_{10}, m_{01}, m_{20}, m_{11}, m_{02}, m_{30}, m_{03}, m_{22}$) were considered to illustrate the case $N = 3$. Whatever the number the nodes, the selected sets chosen to illustrate the effect of N were symmetric, allowing treating both properties equally. Additionally, the results obtained with the discrete solution of the PBE are also reported on Fig. 3.

The mixed moments of global order 0, 1 or 2 are quite similar whatever the number of nodes and equal to the moments calculated from the discrete solution. Significant differences are observed, above all for a number of nodes equal to 2 compared to the other cases. For N larger than 2, an effect of the number of nodes on the results is only observed for mixed moments having a high order with respect to the second variable. The accuracy of the predictions can also be evaluated comparing the results with the moments calculated from the discrete solution. Table 3 reports the errors (percentage of the difference between the DQMOM and discrete solution over the discrete solution) on some mixed moments calculated at the initial time and after 50 min of the process. Best agreement between DQMOM and discrete solutions are obtained with a number of nodes equal to 3 or 4 depending on the mixed moment considered. In that case, the values calculated with the discrete solution are over or under predicted with DQMOM with an error less than 20% (excepted for m_{03} and m_{04}). Remembering that the discrete solute may also introduce approximations in the results because of a limited number of discrete intervals considered, the accuracy of DQMOM method with a number of nodes equal to 3 or 4 may be said reasonably correct.

In order to complete this analysis, the change of the predictions of some specific mixed moments versus time have been reported on Fig. 4 for different values of N. In the case of N equal to 3, the results obtained with the different sets discussed earlier have also been reported. It can be concluded that the effect of number of nodes on the result is more important than the effect of the selected set for a given number of nodes. Indeed the curves corresponding to the different selected sets for $N = 3$ are placed between the ones obtained for $N = 2$ and $N = 4$. Globally, the differences remain slight above all chosen a number of nodes equal to 3 or 4.

Moreover, as reported by Frances and Liné [25], the change over the first minutes of the process of the dimensionless moments (obtained dividing the transient moments by their initial values) in a monovariate model can be interpreted in order to evaluate the process time-scale. It was shown that the size reduction time-scale was correlated with the time-scale of the local disintegration phenomena (equal to 2 min in the present studied case). A similar analysis can be done in a bivariate model considering the pure mixed moments with respect to the two properties. The following equations have be derived from the first five minutes of the process:

$$\frac{m_{k0}(t)}{m_{k0}(0)} = exp\left(-\frac{t}{\tau_k}\right) \quad (20)$$

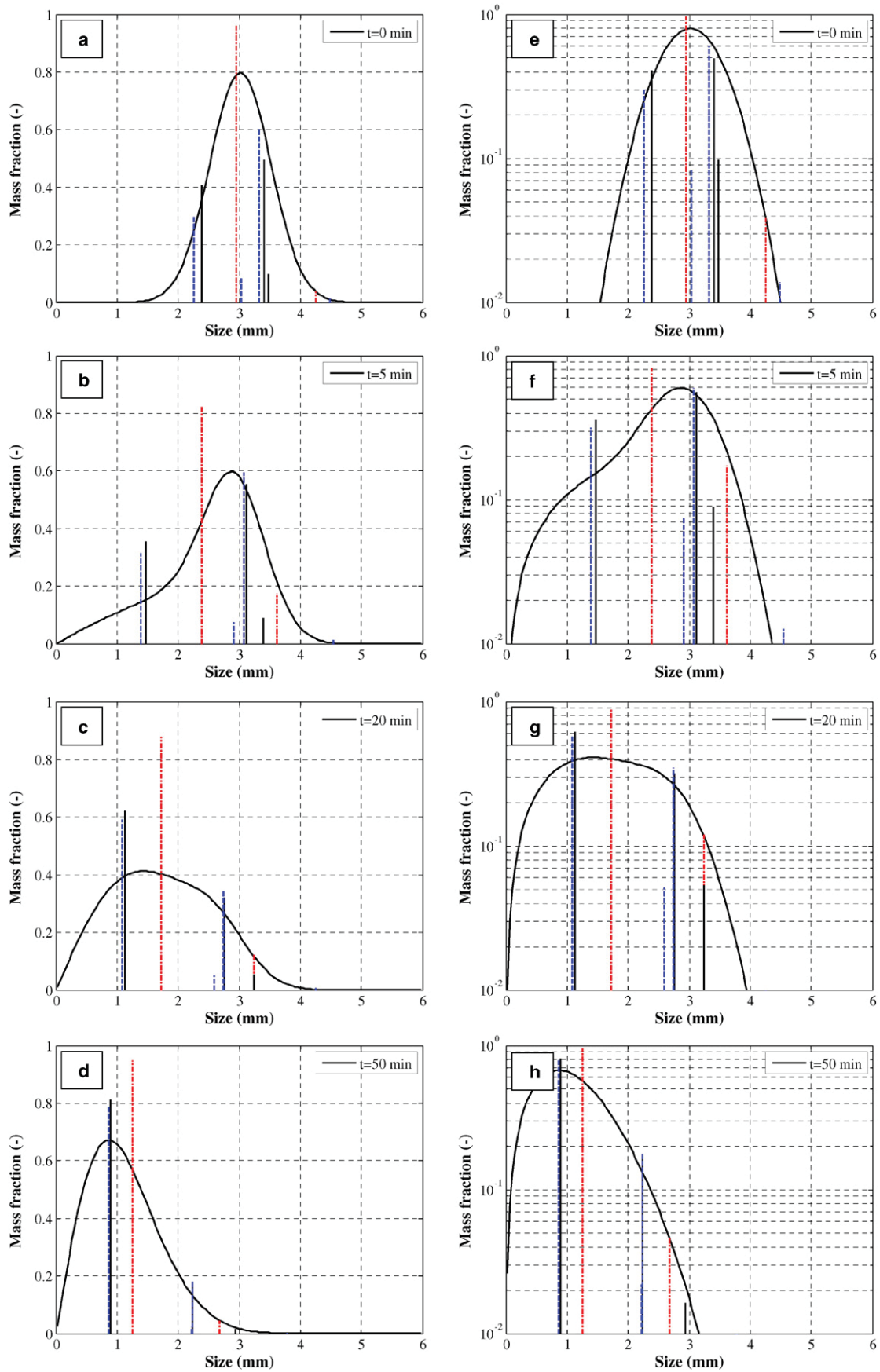$$\frac{m_{0l}(t)}{m_{0l}(0)} = exp\left(-\frac{t}{\delta_l}\right) \quad (21)$$

Fig. 5. Visualization on monovariate PSD of the couples (w,x) obtained by DQMOM with different numbers of nodes ($N=2$ dashdot red lines, $N=3$ solid black lines, $N=4$ dashed blue lines).
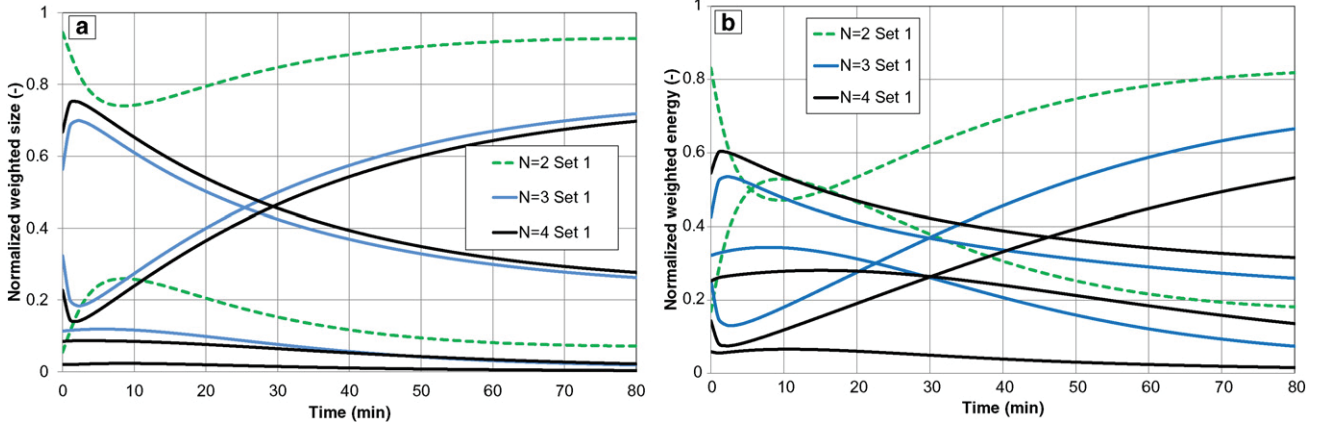
Fig. 6. Effect of the number of nodes on normalized weighted size (a) and energy (b).

in which τ_k and δ_l are the process time-scales respectively to the first and the second property. The corresponding values are reported in Table 4 for different numbers of nodes.

The decrease of pure mixed moments related to the first internal co-ordinate versus time is coherent with a particle size decrease (pure breakage process). The time-scale of the process always exceeded the time-scale of the local disintegration process. Furthermore, the values of the size reduction time-scale are nearly the same when the number of nodes are equal to 3 or 4 and slightly differ to the ones obtained with a number of nodes equal to 2. Concerning the change versus time of the dimensionless pure moments with respect to the second property, their decrease is coherent with a decrease of the energy needed for breakage as the particle size decreases. The values of the energy reduction time-scale recovered for a number of nodes equal to 3 or 4 are also rather similar. When the number of nodes is equal to 2, the values obtained are significantly different for δ_1 and δ_2 and the Eq. (21) is even no more valid for the dimensionless pure moments of a global order greater than 2. The agreement of the results using $N = 3$ or 4 if thus also confirm considering the kinetic parameters of the grinding process.

3.3. Visualization of DQMOM weights and abscissas on particle distribution

The DQMOM approach provides access to the change of the weights and abscissas versus time. These data are not directly correlated to the particle size-energy distribution but additional information can be drawn visualizing theses values on the particle distribution for the different conditions. The monovariate particle distributions considering the particle size as the property for the solid phase were obtained using a discrete solution of the population balance equation. Using the discrete solution of the particle size-energy distribution, the monovariate distributions $f(x,t)$ was then derived calculating the mean values of the mass fractions over the energy range. The particle size distributions are reported on Fig. 5 (on a linear scale from Fig. 5a to d and on a semi-log scale from Fig. 5e to h) for four different characteristic times. The couples (w,x) obtained with DQMOM and different numbers of nodes ($N = 2, 3$ or 4) have also been reported on these graphs. The particle size distributions (PSD) shown on Fig. 5a to d are rather typical of a size-reduction process. Indeed, the PSD, which is initially narrow, spreads over time with the appearance of a sub-population of fragments and then turns again monomodal as the sub-population of the large particles disappears and the finer population becoming predominant. Whatever the number of nodes considered, the values and the changes of the size-abscissas versus time are in good agreement with the particle size curves. The abscissas with the highest weights correspond to the modes of the distributions (more (or most) probable particle size(s) for momomodal (or multimodal) distributions). It can be observed that the results obtained with a number of

nodes equal to 3 or 4 are rather similar. Indeed, two of the abscissas having the highest weights have nearly the same values and the gap between them even decreases versus time. The "remaining part" of the distributions is distributed on the third abscissa for $N = 3$ or the third and the fourth abscissas for $N = 4$. It is also clear on these graphs that a fourth abscissa is not really needed since the corresponding weight is very low whatever the time considered and even when the PSD is bimodal. On the contrary, a number of nodes equal to two leads to different values for the abscissas compared to the other cases and only two abscissas also seem not to be enough to properly reproduce PSD.

Theoretically, the same analysis could be done on the particle energy distributions. However, in that case, using the discrete solution of the particle size-energy distribution, identical monovariate energy distribution curves $f(e,t)$ would be obtained whatever the time considered since the energy spectrum was assumed to be independent of time in the present studied case. Indeed the dependence of the energy spectrum on the particle size vanishes when mean values of the mass fractions are calculated over the entire size range. On the opposite, on the bivariate approach, the energy-abscissas change versus time because they are linked to the particle size distribution through the Gauss approximation and a direct comparison cannot be made.

So an alternative analysis is proposed on Fig. 6 where the normalized weighted abscissas (defined by the ratio of the weighted abscissa on the sum of all the weighted abscissas) have been reported versus the process time. It can be first observed on Fig. 6a that the normalized weighted size curves predicted by DQMOM with $N = 3$ are rather similar to the first three normalized ones predicted with $N = 4$. Two of these curves have reflected patterns versus time. The first normalized weighted size curve represents the evolution of the normalized length of the intermediate-size population which increases first because of the breakage of the coarser particles and decreases then producing finer fragments. Inversely, the second normalized value expresses the length of the finer population. It decreases first, because their characteristic size sharply decreases, and increases then because of the increase of the proportion of fine particles. The evolution of the length of the coarse particles, always decreasing versus time, is represented by the third curve when $N = 3$ and by the third and the fourth ones when $N = 4$. As already mentioned above, the fourth term keeps low value all along the process and it does not seem really useful in the breakage description. It is also clear on Fig. 6a that the normalized weighted size values predicted with $N = 2$ are completely different to the ones obtained with a higher number of nodes.

Concerning the change versus time of the normalized weighted energy reported on Fig. 6b, similar comments can be done, which is not surprising since the energy needed for breakage is correlated with the particle size. Although the differences between the curves predicted with $N = 3$ and $N = 4$ seem to be more important than on Fig. 6a, the same trends versus time and the same similarities taking $N = 3$ or $N = $

4 are observed. On the contrary, with $N = 2$ the curves have complete different patterns.

4. Conclusions

The DQMOM approach was used to solve a bivariate population balance equation applied to a grinding process in which the particles are simultaneously characterized by their size and the minimum energy needed for their breakage. The mixed moments of the energy-size distribution are expressed by the quadrature form of the population density defined for a given number of nodes and incorporating the weights and the abscissas defined for each solid property. We discuss in this paper the effect of the number of nodes and the selected set of moments needed to solve the system on the accuracy of the results. The method allows predicting the transient change of the mixed moments which were compared to the values derived from a discrete solution of the PBE considering a finite number of size and energy intervals. The model must be initialized by the weights and abscissas corresponding to the initial particle distribution. For that purpose, a squared mean method has been implemented to solve the non-linear system constituted by the initial mixed moments. For a given number of nodes, the values of the weights and abscissas can slightly differ depending on the selected set of moments and consequently the initial mixed moments are not exactly the same. The choice of moments set also affects the precision of the moments predicted versus time but above all the values of the mixed moments for which the global order is high and more particularly in the studied case for those having a high order with respect to the second property. This result must be put in relation with the respective range of variation of the two properties. The most discrepancy between predicted values occurs for the moments which are not included in the selected set. Moreover, the mixed moments of global order 0, 1 or 2 are quite similar whatever the number of nodes and equal to the moments calculated from the discrete solution. Significant differences are observed for the moments with a higher order and above all for a number of nodes equal to 2. A good agreement between DQMOM and discrete solutions are obtained with a number of nodes equal to 3 or 4 depending on the mixed moment considered. It was also concluded that the effect of the number of nodes on the results is more important than the effect of the selected set for a fixed number of nodes. Finally, it was observed that the values and the changes of the size-abscissas versus time are well correlated with the particle size distribution, calculated from the discrete solution, considering mean values of the mass fractions over the entire energy range. Two abscissas (when the number of nodes is equal to 2) are not enough to represent properly bimodal distributions but three abscissas for $N = 3$ or $N = 4$ give satisfactory results. The fourth abscissa for $N = 4$ is not really needed since the corresponding weight always remains very low. Consequently the normalized weighted size and energy curves predicted by DQMOM with $N = 3$ are rather similar to the first three normalized curves predicted with $N = 4$. That result confirms that the DQMOM approach, choosing a number of nodes equal to 3, associated with a smart selection of moment set, incorporating all moments of interest, is able to predict in an efficient way the changes of a bivariate distribution during a grinding process.

References

[1] F. Gelbard, J.H. Seinfeld, Numerical solution of the dynamic equation for particulate systems, J. Comput. Phys. 28 (1978) 357–375.
[2] M.J. Hounslow, R.L. Ryall, V.R. Marshall, A discretized population balance for nucleation, growth and aggregation, AICHE J. 34 (1988) 1821–1832.
[3] D. Ramkrishna, Population Balances — Theory of Particulate Processes, Academic Press, San Diego, 2000.
[4] B. Scarlett, Particle populations — to balance or not to balance, that is the question! Powder Technol. 125 (2002) 1–4.
[5] A.H. Alexopoulos, C. Kiparissides, Solution of the bivariate dynamic population balance equation in batch particulate systems: combined aggregation and breakage, Chem. Eng. Sci. 62 (2007) 5048–5053.
[6] A.H. Alexopoulos, A. Roussos, C. Kiparissides, Dynamic evolution of the multivariate particle size distribution undergoing combined particle growth and aggregation, Chem. Eng. Sci. 64 (2009) 3260–3269.
[7] W. Heineken, D. Flockerzi, A. Voigt, K. Sundmacher, Dimension reduction of bivariate population balances using the quadrature method of moments, Comput. Chem. Eng. 35 (2011) 50–62.
[8] F. Puel, G. Fevotte, J.-P. Klein, Simulation and analysis of industrial crystallization processes through multidimensional population balance equations. Part 2: a study of semi-batch crystallization, Chem. Eng. Sci. 58 (2003) 3729–3740.
[9] Y. Zhang, M.F. Doherty, Simultaneous prediction of crystal shape and size for solution crystallization, AICHE J. 50 (2004) 2101–2112.
[10] C.Y. Ma, X.Z. Wang, K.J. Roberts, Multi-dimensional population balance modeling of the growth of rod-like L-glutamic acid crystals using growth rates estimated from in-process imaging, Adv. Powder Technol. 18 (2007) 707–723.
[11] D.L. Marchisio, On the use of bi-variate population balance equations for modelling barium titanate nanoparticle precipitation, Chem. Eng. Sci. 64 (2009) 697–708.
[12] B. Niemann, K. Sundmacher, Nanoparticle precipitation in microemulsions: population balance model and identification of bivariate droplet exchange kernel, J. Colloid Interface Sci. 342 (2010) 361–371.
[13] C.D. Immanuel, F.J. Doyle, Solution technique for a multi-dimensional population balance model describing granulation processes, Powder Technol. 156 (2005) 213–225.
[14] D.L. Wright, R. McGraw, D.E. Rosner, Bivariate extension of the quadrature method of moments for modeling simultaneous coagulation and sintering particle populations, J. Colloid Interface Sci. 236 (2001) 242–251.
[15] C. Kirse, H. Briesen, Numerical solution of mixed continuous-discrete population balance models for depolymerisation of branched polymers, Comput. Chem. Eng. 73 (2015) 154–171.
[16] L.M. Tavares, R.P. King, Single-particle fracture under impact loading, Int. J. Miner. Process. 54 (1998) 1–28.
[17] R.P. King, F. Bourgeois, Measurement of fracture energy during single-impact fracture, Miner. Eng. 6 (1993) 353–367.
[18] S. Romeis, J. Paul, P. Herre, M. Hanisch, R.N. Klupp Taylor, J. Schmidt, W. Peukert, In situ deformation and breakage of silica particles inside a SEM, Procedia Eng. 102 (2015) 201–210.
[19] R.O. Fox, Bivariate direct quadrature method for coagulation and sintering of particle populations, Aerosol Sci. 37 (2006) 1562–1580.
[20] D.L. Marchisio, R.O. Fox, Solution of population balance equations using the direct quadrature method of moments, J. Aerosol Sci. 36 (2005) 43–73.
[21] A. Zucca, D.L. Marchisio, M. Vanni, A.A. Barresi, Validation of bivariate DQMOM for nanoparticle processes simulation, AIChE J 53 (4) (2007) 918–931.
[22] D.L. Marchisio, R.O. Fox, Computational Models for Polydisperse Particulate and Multiphase Systems, Cambridge University Press, 2013.
[23] E.F. Crespo, Application of particle fracture energy distributions to ball milling kinetics, Powder Technol. 210 (2011) 281–287.
[24] C. Yuan, R.O. Fox, Conditional quadrature method of moments for kinetic equations, J. Comput. Phys. 230 (2011) 8216–8246.
[25] C. Frances, A. Liné, Comminution process modeling based on the monovariate and bivariate direct quadrature method of moments, AIChE J. 60 (5) (2014) 1621–1631.
[26] R.G. Gordon, Error bounds in equilibrium statistical mechanics, J. Math. Phys. 9 (5) (1968) 655–663.
[27] R.O. Fox, Optimal moment sets for multivariate direct quadrature method of moments, Ind. Eng. Chem. Res. 48 (2009) 9686–9696.